

Global Volumetric Phase Fractions in Horizontal Three-Phase Flows

R. T. Lahey, Jr., M. Açıkgöz, and F. França

Center for Multiphase Research, Rensselaer Polytechnic Institute, Troy, New York 12180

Generalized drift-flux expressions for horizontal three-phase (gas/water/oil) conduit flows have been derived. A detailed set of phasic volume fraction data were measured for the various flow regimes observed in air/water/oil flows. This article shows that drift-flux techniques can be used to predict the phasic volumetric fractions for horizontal three-phase flows, such as those which may occur in off-shore oil well lines.

Introduction

Drift-flux models (Zuber and Findlay, 1965) were developed to account for the effect of nonuniform lateral-phase distribution and the local relative velocity between two phases. They have been widely used in two-phase analyses since they can successfully predict the global volumetric phase fractions for steady and quasi-steady vertical two-phase flows. The drift-flux parameters are known to be a function of flow regime, conduit size, and operating conditions (for example, pressure). Nevertheless, for a particular situation they correlate two-phase data remarkably well.

Recently, drift-flux models have been extended to horizontal two-phase flows (França et al., 1992), where it was shown that, contrary to popular belief, the drift velocity may not be negligible for horizontal flows. In addition, Bhaga and Weber have proposed a generalized drift-flux model for the vertical three-phase flow of gas/liquid/solid mixtures, and this model was verified against their experimental data.

The prediction of the global volumetric phase fractions in horizontal three-phase gas/water/oil flow is important because of its application to off-shore oil well technology, however it is a challenging task because of the rich variety of flow regimes which may occur (Açıkgöz et al., 1992). In three-phase flows, involving two immiscible liquids, not only do the gas-phase distribution parameter and drift velocity have to be determined, but also those for the dispersed liquid component in the continuous liquid phase of the flowing immiscible liquid/liquid mixture.

In spite of many applications in the petroleum and chemical industries of three-phase flows having two immiscible liquid components, there have been only a few attempts to model

flow-regime-specific phenomena. In a previous study, Tek (1961) considered the two immiscible liquid components to be a single-liquid phase having mixture properties. His approach did not take the effects of the different liquid/liquid flow regimes into account, thus limiting its applicability to a small range of operating conditions. Later, Galyamov et al. (1971)

Table 1a. Global Volumetric Phase Fraction Data, Water-Based Dispersed Slug Flow (Region-7)

$\langle j_g \rangle$ (m/s)	$\langle j_w \rangle$ (cm/s)	$\langle j_o \rangle$ (cm/s)	$\langle \alpha_g \rangle$	$\langle \alpha_w \rangle$	$\langle \alpha_o \rangle$
6.623	45.502	15.571	0.718	0.221	0.061
8.831	65.974	15.571	0.718	0.230	0.052
9.935	65.974	2.356	0.856	0.129	0.015
2.208	55.403	4.363	0.693	0.269	0.038
2.760	55.403	4.363	0.653	0.328	0.019
1.104	12.584	4.363	0.708	0.250	0.042
0.552	12.584	4.363	0.674	0.278	0.048
0.828	12.584	4.363	0.653	0.288	0.059
1.380	12.584	4.363	0.762	0.194	0.044
1.656	12.584	4.363	0.643	0.292	0.065
2.208	55.403	4.363	0.578	0.384	0.038
1.104	12.584	4.363	0.724	0.230	0.046
2.208	55.403	4.363	0.597	0.365	0.038
2.760	55.403	4.363	0.703	0.268	0.029
2.208	55.403	4.363	0.687	0.278	0.035
0.552	12.584	4.363	0.681	0.269	0.050
0.828	12.584	4.363	0.664	0.278	0.058
1.380	12.584	4.363	0.770	0.188	0.042
1.656	12.584	4.363	0.651	0.288	0.061
4.278	22.888	8.013	0.809	0.137	0.054
4.967	36.269	12.774	0.677	0.247	0.076
7.617	51.362	20.289	0.705	0.208	0.087

Current Address of F. França: Depto. De Energia—F.E.C., UNICAMP, 13081 Campinas—S.P., Brazil.

Table 1b. Global Volumetric Phase Fraction Data, Water-Based Stratified/Wavy & Incipient Annular Flows (Regions-8&9)

$\langle j_a \rangle$ (m/s)	$\langle j_w \rangle$ (cm/s)	$\langle j_o \rangle$ (cm/s)	$\langle \alpha_a \rangle$	$\langle \alpha_w \rangle$	$\langle \alpha_o \rangle$
4.416	4.338	2.356	0.775	0.192	0.033
10.211	5.663	8.013	0.860	0.069	0.071
9.935	65.974	2.356	0.856	0.129	0.015
13.247	5.663	4.363	0.900	0.061	0.039
13.247	7.285	4.363	0.900	0.065	0.035
14.902	5.663	4.363	0.906	0.058	0.036
2.208	65.974	4.363	0.693	0.274	0.033
2.760	65.974	4.363	0.689	0.282	0.029
3.312	65.974	4.363	0.651	0.328	0.021
3.864	65.974	4.363	0.664	0.311	0.025
5.519	65.974	4.363	0.703	0.276	0.021
2.760	55.403	4.363	0.653	0.328	0.019
3.312	55.403	4.363	0.682	0.301	0.017
3.864	55.403	4.363	0.597	0.345	0.058
4.416	55.403	4.363	0.597	0.365	0.038
2.208	5.663	4.363	0.808	0.148	0.044
2.208	8.570	4.363	0.758	0.198	0.044
2.760	55.403	4.363	0.695	0.280	0.025
10.211	5.663	10.254	0.777	0.083	0.140
8.279	8.570	14.138	0.745	0.104	0.151
8.279	8.570	17.074	0.737	0.098	0.165
6.623	22.888	9.099	0.810	0.159	0.031
8.279	11.219	9.099	0.822	0.119	0.059
9.935	5.663	14.138	0.812	0.059	0.129
8.279	8.570	9.099	0.820	0.092	0.088
6.623	27.705	9.099	0.766	0.173	0.061
6.623	45.502	23.782	0.695	0.200	0.105
8.279	27.705	23.782	0.718	0.153	0.129
11.260	41.728	2.356	0.780	0.213	0.007
13.247	55.403	9.099	0.787	0.179	0.034

Table 1c. Global Volumetric Phase Fraction Data, Water-Based Dispersed Annular Flow (Region-10)

$\langle j_a \rangle$ (m/s)	$\langle j_w \rangle$ (cm/s)	$\langle j_o \rangle$ (cm/s)	$\langle \alpha_a \rangle$	$\langle \alpha_w \rangle$	$\langle \alpha_o \rangle$
13.247	11.219	4.363	0.900	0.090	0.010
10.211	5.663	8.013	0.860	0.069	0.071
9.935	27.705	15.571	0.816	0.142	0.042
13.247	19.810	9.099	0.860	0.081	0.059
13.247	13.976	4.363	0.877	0.102	0.021
13.247	19.810	4.363	0.885	0.096	0.019
13.247	27.705	4.363	0.868	0.100	0.032
13.247	36.269	4.363	0.864	0.109	0.027
13.247	45.502	4.363	0.839	0.142	0.019
13.247	55.403	4.363	0.824	0.163	0.013
13.247	65.974	4.363	0.818	0.167	0.015
14.902	7.285	4.363	0.904	0.061	0.035
16.558	5.663	4.363	0.910	0.056	0.034
14.902	18.311	9.099	0.871	0.102	0.027
16.558	21.336	9.099	0.889	0.090	0.021
8.831	45.502	9.099	0.780	0.182	0.038
13.247	21.336	9.099	0.864	0.107	0.029
13.247	8.570	9.099	0.881	0.079	0.040
14.902	21.336	9.099	0.862	0.109	0.029
8.831	65.974	9.099	0.799	0.180	0.021
13.247	11.219	9.099	0.889	0.090	0.021
16.558	27.705	9.099	0.850	0.121	0.029

Table 1d. Global Volumetric Phase Fraction Data, Oil-Based Dispersed Plug Flow (Region-1)

$\langle j_a \rangle$ (m/s)	$\langle j_w \rangle$ (cm/s)	$\langle j_o \rangle$ (cm/s)	$\langle \alpha_a \rangle$	$\langle \alpha_w \rangle$	$\langle \alpha_o \rangle$
0.414	3.014	9.099	0.442	0.086	0.472
0.414	5.001	9.099	0.392	0.186	0.422
0.414	1.689	9.099	0.438	0.069	0.493
0.414	0.364	9.099	0.440	0.029	0.531
0.414	12.584	23.782	0.309	0.204	0.487
0.414	7.928	23.782	0.319	0.132	0.549
0.414	4.338	23.782	0.336	0.077	0.587
0.359	4.814	10.254	0.361	0.232	0.407
0.414	1.104	15.571	0.373	0.138	0.489
0.386	1.380	18.647	0.324	0.136	0.540

Table 1e. Global Volumetric Phase Fraction Data, Oil-Based Dispersed Slug Flow (Region-2)

$\langle j_a \rangle$ (m/s)	$\langle j_w \rangle$ (cm/s)	$\langle j_o \rangle$ (cm/s)	$\langle \alpha_a \rangle$	$\langle \alpha_w \rangle$	$\langle \alpha_o \rangle$
0.552	9.881	9.099	0.327	0.138	0.535
0.552	9.881	12.774	0.319	0.109	0.572
0.414	3.014	9.099	0.442	0.086	0.472
1.104	3.014	9.099	0.478	0.121	0.401
0.414	5.001	9.099	0.392	0.186	0.422
0.414	1.689	9.099	0.438	0.069	0.493
0.414	0.364	9.099	0.403	0.029	0.568
0.414	12.584	23.782	0.309	0.204	0.487
0.414	7.928	23.782	0.319	0.132	0.549
2.760	3.279	23.782	0.426	0.073	0.501
2.708	3.543	23.782	0.384	0.077	0.539

Table 1f. Global Volumetric Phase Fraction Data, Oil-Based Stratified/Wavy Flows (Regions-3&4)

$\langle j_a \rangle$ (m/s)	$\langle j_w \rangle$ (cm/s)	$\langle j_o \rangle$ (cm/s)	$\langle \alpha_a \rangle$	$\langle \alpha_w \rangle$	$\langle \alpha_o \rangle$
4.416	1.689	2.356	0.787	0.111	0.102
10.211	5.663	8.013	0.860	0.069	0.071
9.935	2.351	2.356	0.870	0.061	0.069
13.247	1.689	4.363	0.781	0.021	0.198
14.902	1.689	4.363	0.824	0.019	0.157
16.558	1.689	4.363	0.829	0.019	0.152
2.208	0.364	4.363	0.693	0.065	0.242
4.416	1.689	3.625	0.701	0.128	0.171
10.211	5.663	10.254	0.777	0.083	0.140
8.279	8.570	14.138	0.745	0.104	0.151
8.279	8.570	17.074	0.737	0.098	0.165
8.279	5.663	9.099	0.701	0.090	0.209
9.935	5.663	9.099	0.812	0.059	0.129
8.279	8.570	23.782	0.779	0.060	0.161
5.519	3.014	9.099	0.597	0.106	0.297
5.519	5.001	9.099	0.576	0.163	0.261
2.760	5.001	9.099	0.538	0.217	0.245
2.760	3.543	9.099	0.530	0.192	0.278
2.760	1.556	9.099	0.534	0.138	0.328
2.760	3.146	4.363	0.574	0.211	0.215
2.760	0.364	4.363	0.551	0.154	0.295
6.623	3.676	4.363	0.634	0.151	0.215
13.247	3.676	4.363	0.733	0.125	0.142
6.623	3.676	9.099	0.616	0.134	0.250
4.416	2.351	6.996	0.589	0.131	0.280
11.260	3.543	14.138	0.748	0.069	0.183
12.584	5.663	15.571	0.814	0.052	0.134
15.896	8.570	20.289	0.841	0.052	0.107

Table 1g. Global Volumetric Phase Fraction Data, Oil-Based Wavy/Stratifying-Annular Flow (Region-5)

$\langle j_a \rangle$ (m/s)	$\langle j_w \rangle$ (cm/s)	$\langle j_o \rangle$ (cm/s)	$\langle \alpha_a \rangle$	$\langle \alpha_w \rangle$	$\langle \alpha_o \rangle$
5.519	3.014	9.099	0.597	0.106	0.297
5.519	5.001	9.099	0.576	0.163	0.261
6.623	5.001	23.782	0.538	0.103	0.359
6.623	3.014	23.782	0.568	0.090	0.342
9.935	3.676	23.782	0.607	0.063	0.330
13.247	4.338	23.782	0.578	0.077	0.345
14.902	3.676	23.782	0.624	0.058	0.318
6.623	3.676	4.363	0.634	0.151	0.215
6.623	3.676	9.099	0.616	0.134	0.250
16.558	3.014	9.099	0.662	0.077	0.261

Table 1h. Global Volumetric Phase Fraction Data, Oil-Based Stratifying-Annular Flow (Region-6)

$\langle j_a \rangle$ (m/s)	$\langle j_w \rangle$ (cm/s)	$\langle j_o \rangle$ (cm/s)	$\langle \alpha_a \rangle$	$\langle \alpha_w \rangle$	$\langle \alpha_o \rangle$
10.221	5.663	8.013	0.860	0.069	0.071
13.247	1.689	4.363	0.781	0.021	0.198
16.558	1.689	4.363	0.829	0.019	0.152
8.279	5.663	10.254	0.693	0.096	0.211
9.935	5.663	9.099	0.777	0.081	0.142
13.246	3.014	9.099	0.724	0.067	0.209
9.935	1.027	4.363	0.722	0.105	0.173
9.935	3.676	4.363	0.718	0.132	0.150
9.935	3.676	4.363	0.722	0.125	0.153
16.558	3.676	4.363	0.743	0.117	0.140
13.247	3.676	4.363	0.733	0.125	0.142
16.558	3.014	9.099	0.662	0.077	0.261

examined the effects of the liquid component volumetric fractions as well as the gas phase's void fraction on the effective viscosity in horizontal pipes. They did not provide a correlation for the phasic volumetric fractions, but noticed that treating the liquid components as a pseudo-single-phase gave dramatically different results as compared to considering them separately. In an interesting, but not well known, study, Shean (1976) attempted to apply drift-flux models to vertical air/water/oil flows to obtain the global volumetric phase fractions. Unfortunately, the drift-flux parameters were not properly defined and thus the results of his study were inconclusive.

The purpose of this article is to show that drift-flux models

can be extended to horizontal gas/water/oil three-phase flows for a wide variety of situations. The three-phase drift-flux model presented herein was developed using experimental data obtained by the authors for horizontal air/water/oil three-phase flow. These data are given in Tables 1 of this paper.

Three-Phase Flow Regimes

Açikgöz et al. (1992) performed extensive flow visualization studies and classified horizontal gas/water/oil three-phase flow

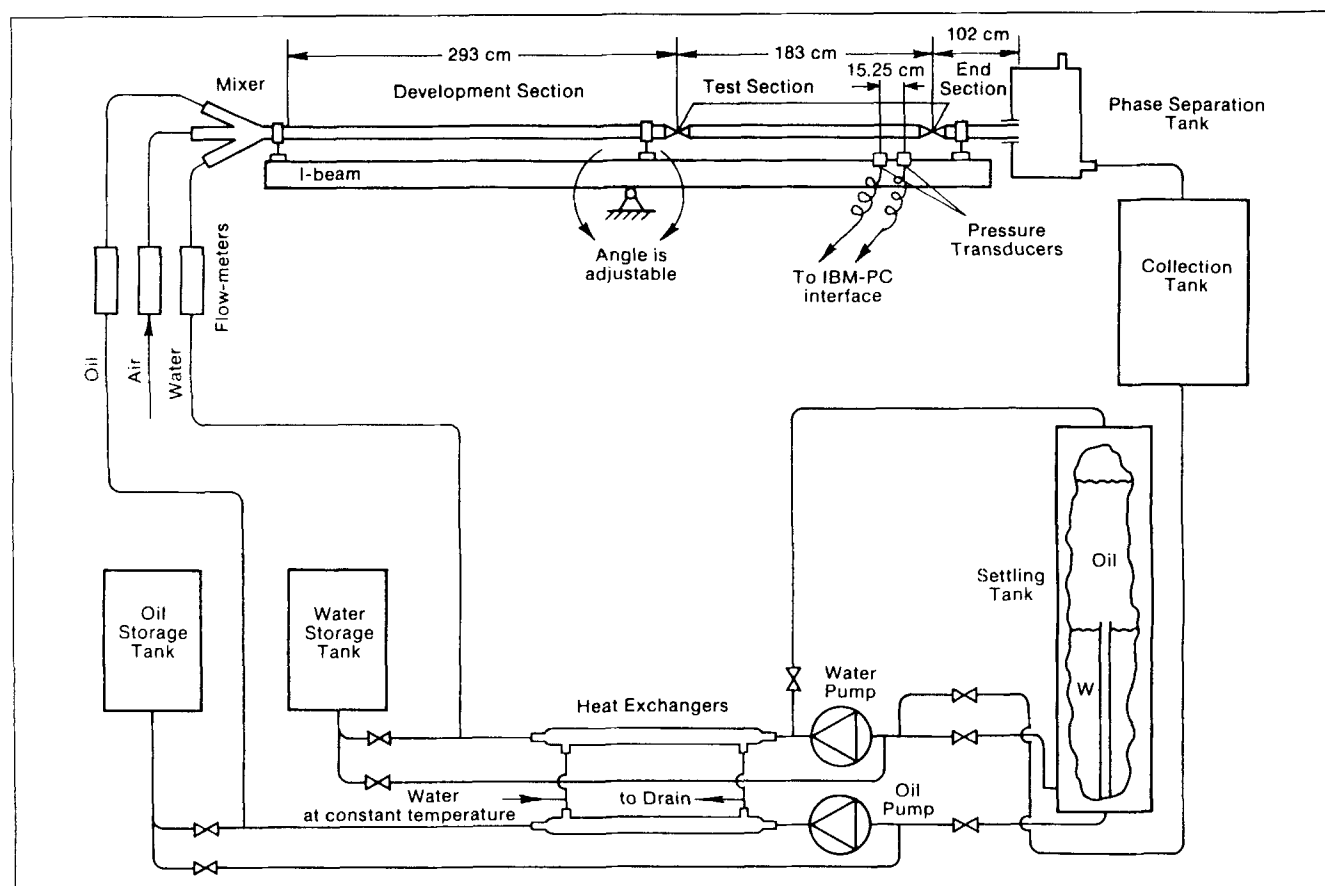


Figure 1. Three-phase flow loop.

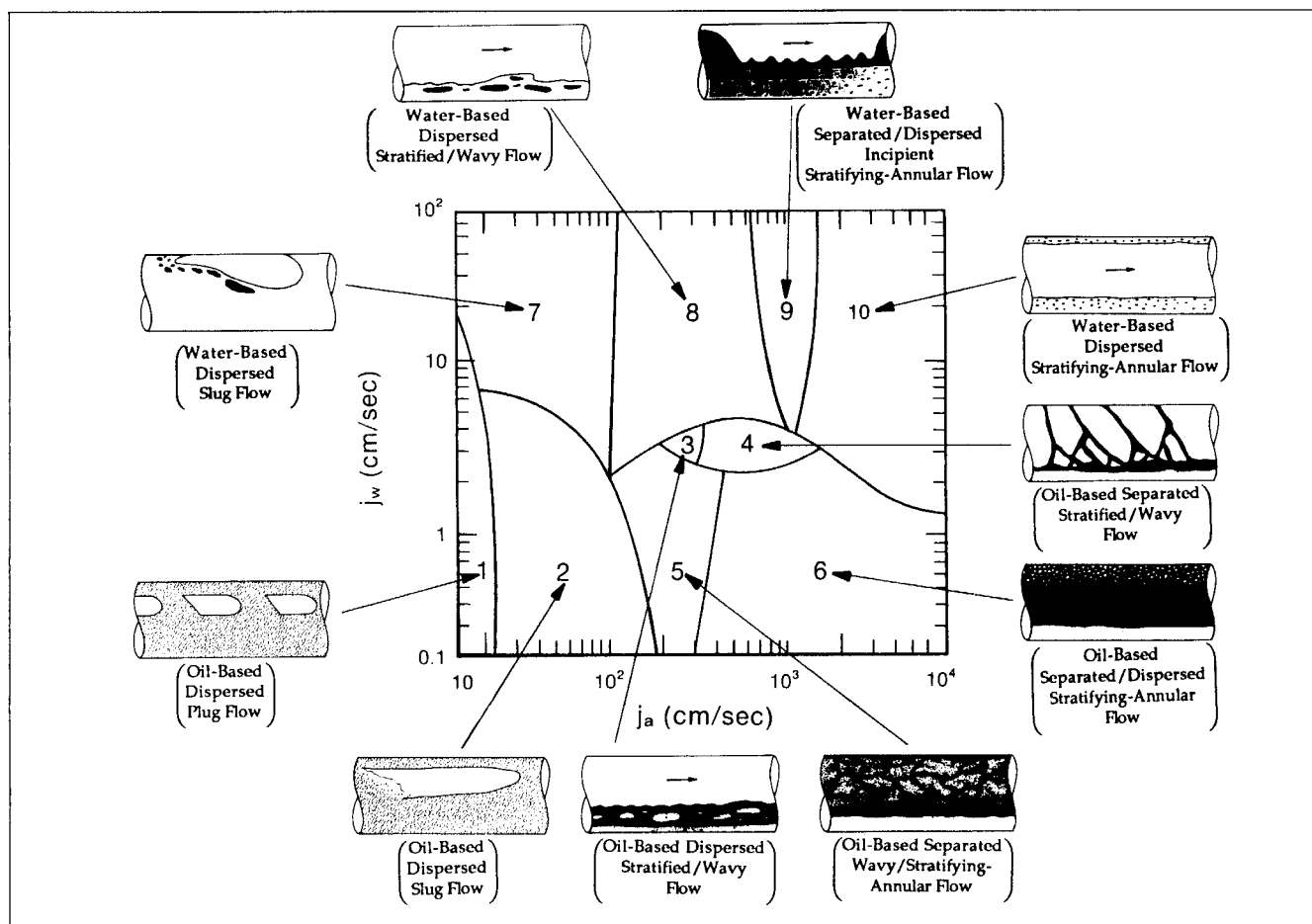


Figure 2. Typical three-phase flow regime map for horizontal oil/water/air flows.

regimes. These data, and those presented herein, were taken in the experimental facility shown schematically in Figure 1. The richness of the resultant flow-regime maps comes from

the many different ways one of the immiscible liquids can be distributed in the continuous liquid phase, as well as the many well-known configurations of the continuous liquid phase with

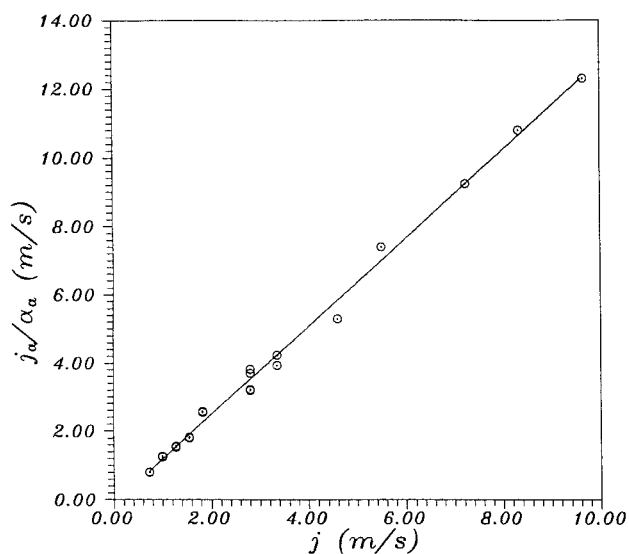


Figure 3. Drift-flux plot, water-based dispersed slug flow, region-7.

($C_d = 1.289$, $V_{aj} = -0.096$ cm/s).

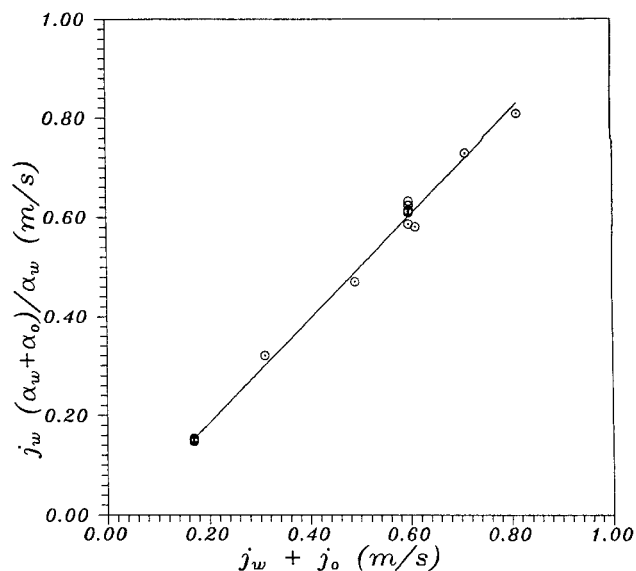


Figure 4. Drift-flux plot, water-based dispersed slug flow, region-7.

($C_w = 1.049$, $V_{wj} = -0.025$ cm/s).

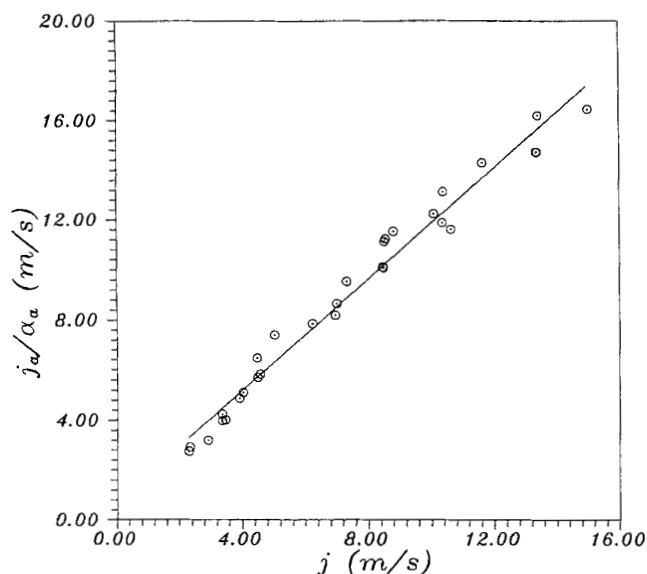


Figure 5. Drift-flux plot for air volumetric fraction: water-based stratified/wavy and incipient annular flows, regions-8&9.

($C_a = 1.115$, $V_{aj} = 0.725$ cm/s).

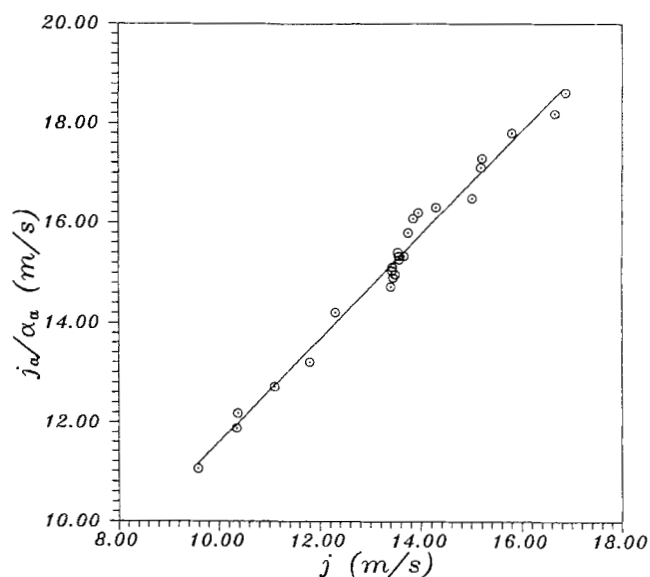


Figure 7. Drift-flux plot, water-based dispersed/annular flow: region-10.

($C_a = 1.041$, $V_{aj} = 1.218$ cm/s).

respect to the gas phase. A typical 3-D flow regime map at a fixed oil superficial velocity (j_o) is shown in Figure 2. Ten distinct flow regimes can be identified in this figure. Since a drift-flux model is known to be flow-regime specific, we expect that the phase distribution parameters (C_a , C_w and C_o) and drift-velocities (V_{aj} , V_{wt} and V_{ot}) will be different for the various flow regimes. A detailed explanation of these parameters and a derivation of the governing drift-flux model are presented later in this paper.

Description of Experiment

The test loop utilized in collecting the global volumetric phase fraction data is shown schematically in Figure 1. Pressurized air, water and mineral oil were chosen as three distinct phases. The mineral oil used in these experiments had a viscosity approximately 116 times higher than that of water (that is, $\mu_o = 0.1164$ Ns/m² at 25°C) and had a density of 864 kg/m³.

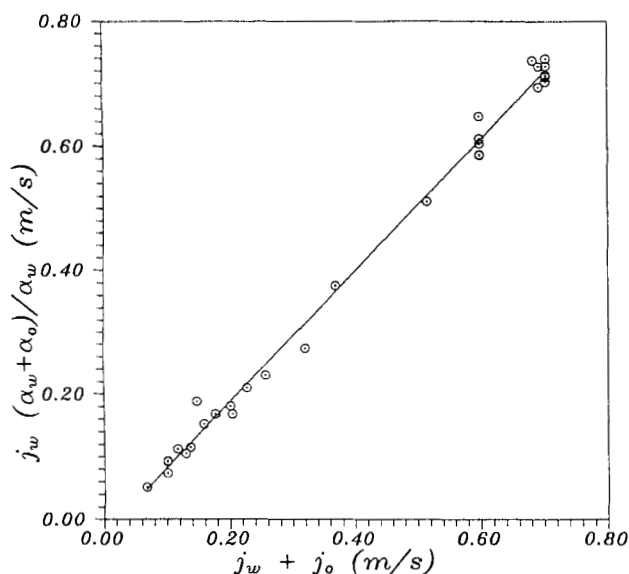


Figure 6. Drift-flux plot, water-based stratified/wavy and incipient annular flows: regions-8&9.

($C_w = 1.056$, $V_{wt} = -0.023$ cm/s).

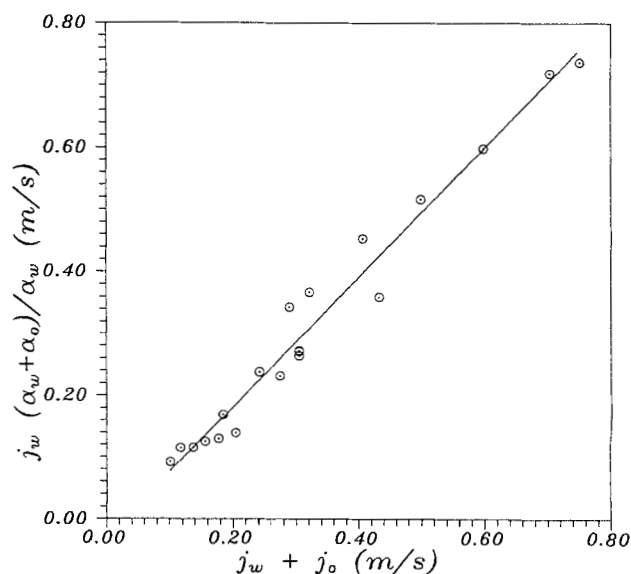


Figure 8. Drift-flux plot, water-based dispersed/annular flow: region-10.

($C_w = 1.047$, $V_{wt} = -0.028$ cm/s).

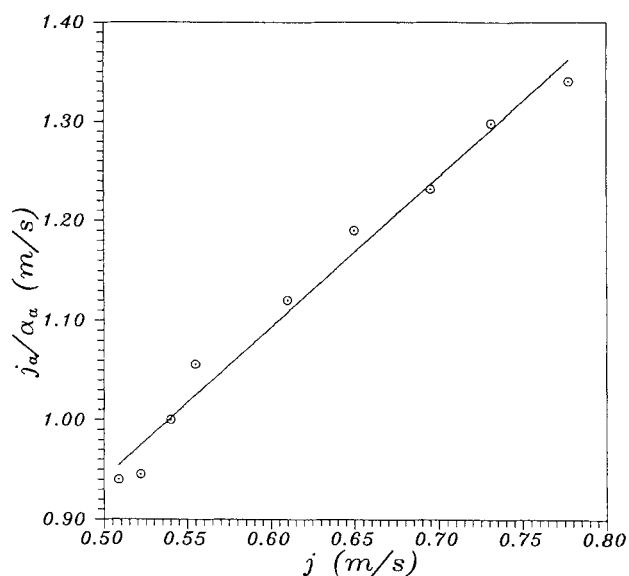


Figure 9. Drift-flux plot, oil-based dispersed plug flow: region-1.

($C_o = 1.514$, $V_{oj} = 0.184$ cm/s).

The flow development and test sections from the three-phase flow mixer to the exit were carefully machined to have a constant inner diameter of 1.9 cm through the copper tubes, ball valves, plexiglas tubes, connectors and unions. Visual observation was possible in the flow development section ($L/D = 154$) and test section ($L/D = 96$) due to the use of plexiglas tubes. Quick-closing valves at both ends of the test section were used to trap the flowing mixture for global volumetric phase fraction measurements. The channel lengths (that is, L/D) were found sufficient for the flow development section to obtain fully-developed flow and for exit section to eliminate end effects, respectively.

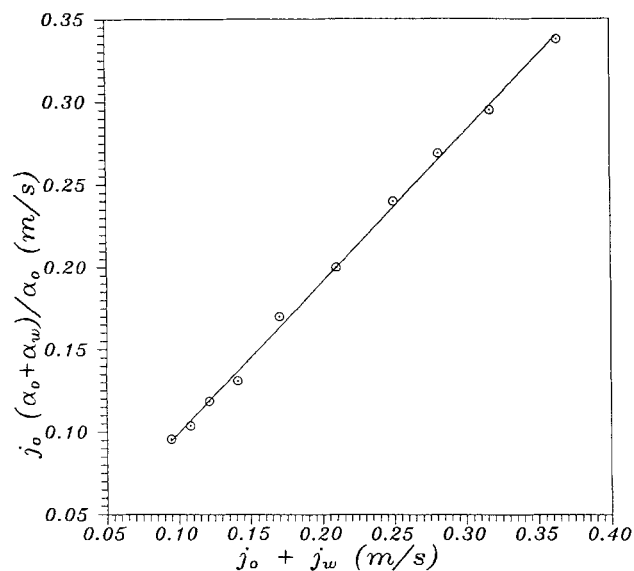


Figure 10. Drift-flux plot, oil-based dispersed plug flow: region-1.

($C_o = 0.914$, $V_{of} = 0.008$ cm/s).

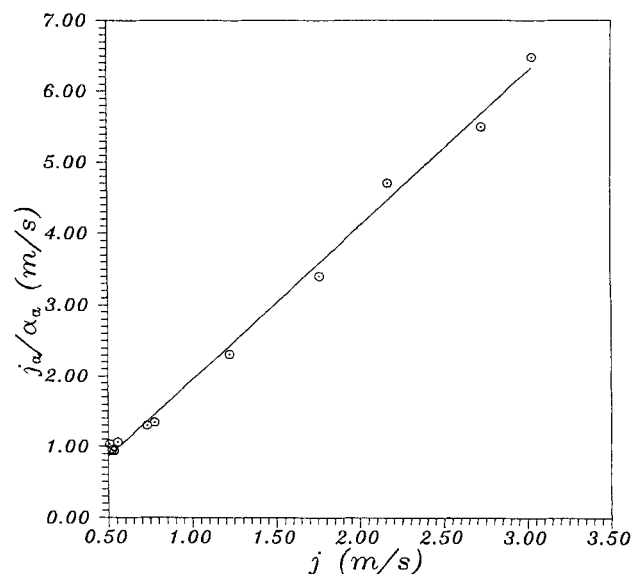


Figure 11. Drift-flux plot, oil-based dispersed slug flow: region-2.

($C_o = 2.328$, $V_{oj} = -0.270$ cm/s).

All of the components between the mixer and phase separation tank were mounted on an I-beam which was pivoted at the middle and supported at the ends. This setup enabled nonhorizontal test section orientations to be achieved, however, in this study only horizontal data were taken.

To eliminate back pressure effects, the exit section was connected to an air separation tank which was open to the atmosphere. A temperature sensor inside of the phase separation tank was used to control cooling water-flow rates to the heat exchangers to keep the three-phase flow loop's water and oil temperatures which entered into the mixer at $26.0 \pm 0.5^\circ\text{C}$.

The liquid phases were routed to a collection tank and trans-

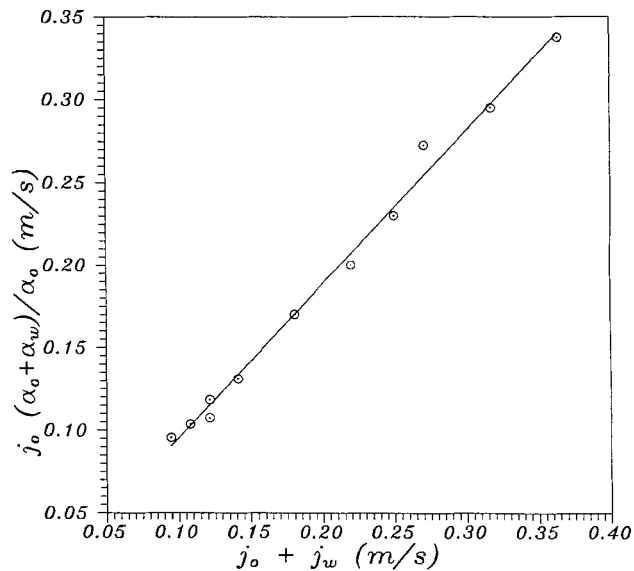


Figure 12. Drift-flux plot, oil-based dispersed slug flow: region-2.

($C_o = 0.938$, $V_{of} = -0.008$ cm/s).

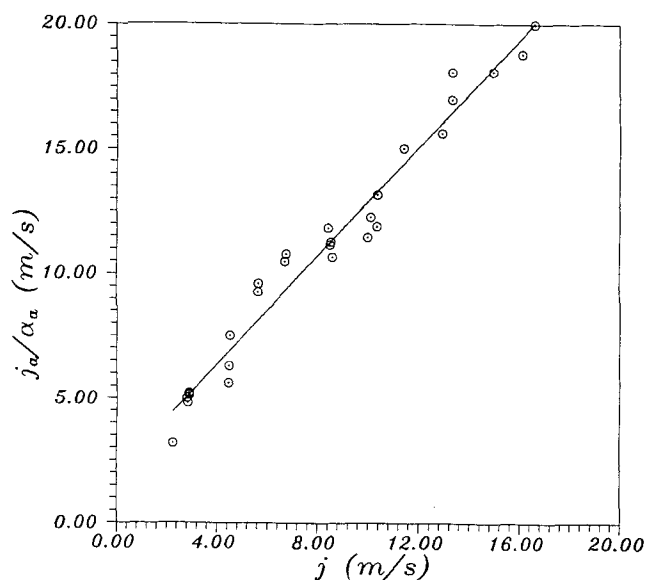


Figure 13. Drift-flux plot, oil-based stratified/wavy flows: regions-3&4.

($C_0 = 1.084$, $V_{oj} = 2.016$ cm/s).

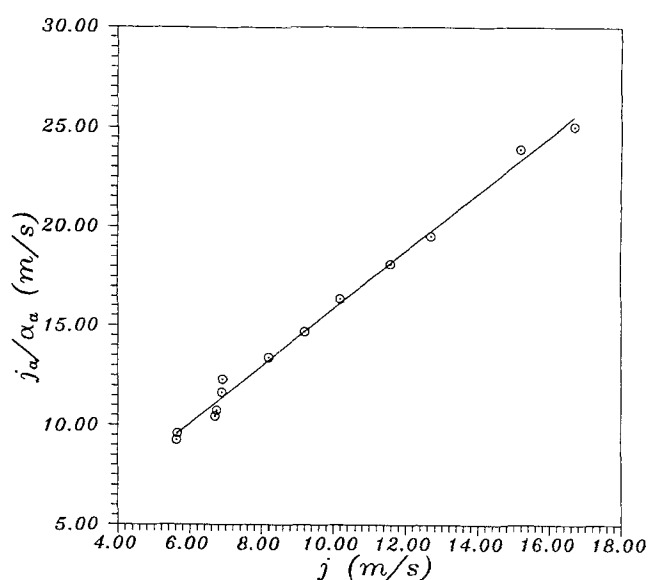


Figure 15. Drift-flux plot, oil-based wavy/stratified-angular flow: region-5.

($C_0 = 1.501$, $V_{oj} = 1.093$ cm/s).

ferred to a 2.7 m tall settling tank after each set of runs, for gravitational phase separation. The maximum time required for the liquid phases to separate for the worst experimental operating conditions (a foamy looking liquid/liquid flow regime) was determined to be approximately six hours. After phase separation, the water and oil were pumped to separate storage tanks having volumes of 75 liters each.

The water and oil were then pumped to the three-phase flow mixer through a parallel connected sets of rotameters for each liquid. Air was also supplied to the mixer at the constant pressure of 414 kPa. The air volumetric flow rate was adjusted by throttle valves and measured by parallel connected air ro-

tameters. Pressures were recorded at the outlet of the air rotameters and at the middle of the test section using Validyne pressure transducers which were connected to an IBM PC through a demodulator and an A/D converter. Pressure data were collected for a specified time interval and were time-averaged for use in the density correction of volumetric air flow rates.

During the global volumetric phase fraction measurement runs, the phasic superficial velocities were adjusted to the desired values, and sufficient time was taken to allow fully developed flow to be established. The linked ball valves at either end of the test section were then closed to get a representative

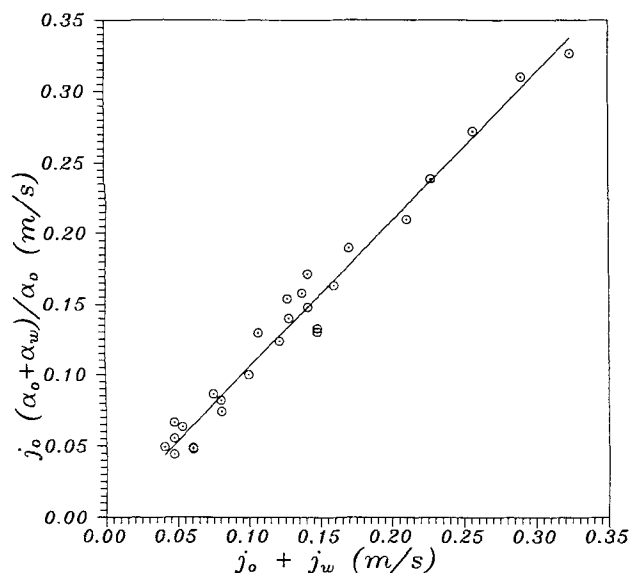


Figure 14. Drift-flux plot, oil-based stratified/wavy flows: regions-3&4.

($C_0 = 1.038$, $V_{oi} = 0.002$ cm/s).

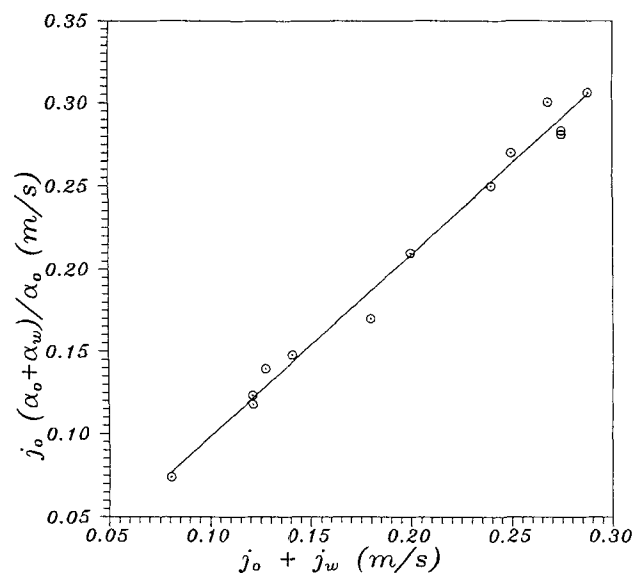


Figure 16. Drift-flux plot, oil-based wavy/stratifying-angular flow: region-5.

($C_0 = 1.084$, $V_{oi} = -0.008$ cm/s).

sample of three-phase flow for global phasic volume fraction measurements. The sample in the isolated test section was then transferred to a graduated cylinder by carefully purging the liquid phases using pressurized air in order to assure not to leave any liquid inside of the test section. The samples of the liquid phases were left in graduated cylinders for a time period of about 10 hours to assure virtually complete gravitational phase separation before measurements of the liquid phase volumes were made. By taking repeated samples it was found that the accuracy of the volume fraction measurements was better than 5% of point (that is, $(\Delta\langle\alpha_k\rangle/\langle\alpha_k\rangle) \leq 0.05$).

Derivation of Drift-Flux Model

As noted previously, a general expression for the global volumetric phase fractions for vertical two-phase flow has been derived by Zuber and Findlay (1965). It will be shown that similar relations are also valid for the gas phase in three-phase (air/water/oil) flow. Thus the global gas volumetric (that is, void) fraction in a three-phase flow can be calculated using the following expression:

$$\frac{\langle j_a \rangle}{\langle \alpha_a \rangle} = C_a \langle j \rangle + V_{aj} \quad (1)$$

where

$$C_a = \frac{\langle \alpha_a j \rangle}{\langle \alpha_a \rangle \langle j \rangle} \quad \text{and} \quad V_{aj} = \frac{\langle \alpha_a (u_a - j) \rangle}{\langle \alpha_a \rangle} \quad (2)$$

and

$$\alpha_a + \alpha_w + \alpha_o = 1 \quad (3)$$

$$j_i = \alpha_i u_i \quad [i = a(\text{air}), w(\text{water}), \text{or}, o(\text{oil})] \quad (4)$$

$$j = j_a + j_w + j_o \quad (5a)$$

$$j_\ell = j_w + j_o \quad (5b)$$

For the flow regimes in which the oil phase is dispersed in the water phase (that is, the water-based flow regime), a relation between the two-liquid phase global volumetric fractions can be derived as follows. First we write an identity for the local parameters:

$$(\alpha_w + \alpha_o)u_w = j_\ell + [(\alpha_w + \alpha_o)u_w - j_\ell] \quad (6)$$

Then

$$\frac{\alpha_w}{\alpha_w + \alpha_o} (\alpha_w + \alpha_o)u_w = \frac{\alpha_w}{\alpha_w + \alpha_o} j_\ell + \frac{\alpha_w}{\alpha_w + \alpha_o} [(\alpha_w + \alpha_o)u_w - j_\ell] \quad (7)$$

hence

$$\alpha_w u_w = \frac{\alpha_w}{\alpha_w + \alpha_o} j_\ell + \left[\alpha_w u_w - \frac{\alpha_w}{\alpha_w + \alpha_o} j_\ell \right] \quad (8)$$

Averaging across the cross-sectional flow area:

$$\langle j_w \rangle = C_w \frac{\langle \alpha_w \rangle}{\langle \alpha_w \rangle + \langle \alpha_o \rangle} \langle j_\ell \rangle + \frac{\langle \alpha_w \rangle}{\langle \alpha_w \rangle + \langle \alpha_o \rangle} V_{w\ell} \quad (9)$$

where

$$C_w = \frac{\left\langle \frac{\alpha_w}{\alpha_w + \alpha_o} j_\ell \right\rangle}{\left[\frac{\langle \alpha_w \rangle}{\langle \alpha_w \rangle + \langle \alpha_o \rangle} \langle j_\ell \rangle \right]} \quad (10a)$$

$$V_{w\ell} = \frac{\left\langle \alpha_w \left(u_w - \frac{j_\ell}{\alpha_w + \alpha_o} \right) \right\rangle}{\left[\frac{\langle \alpha_w \rangle}{\langle \alpha_w \rangle + \langle \alpha_o \rangle} \right]} \quad (10b)$$

Finally, using Eq. 5b, we obtain:

$$\frac{\langle j_w \rangle}{\left[\frac{\langle \alpha_w \rangle}{\langle \alpha_w \rangle + \langle \alpha_o \rangle} \right]} = C_w (\langle j_w \rangle + \langle j_o \rangle) + V_{w\ell} \quad (11)$$

A similar expression can also be derived for oil-based flow regimes:

$$\frac{\langle j_o \rangle}{\left[\frac{\langle \alpha_o \rangle}{\langle \alpha_o \rangle + \langle \alpha_w \rangle} \right]} = C_o \langle j_\ell \rangle + V_{o\ell} \quad (12)$$

where

$$C_o = \frac{\left\langle \frac{\alpha_o}{\alpha_o + \alpha_w} j_\ell \right\rangle}{\left[\frac{\langle \alpha_o \rangle}{\langle \alpha_o \rangle + \langle \alpha_w \rangle} \langle j_\ell \rangle \right]} \quad (13a)$$

$$V_{o\ell} = \frac{\left\langle \alpha_o \left(u_o - \frac{j_\ell}{\alpha_o + \alpha_w} \right) \right\rangle}{\left[\frac{\langle \alpha_o \rangle}{\langle \alpha_w \rangle + \langle \alpha_o \rangle} \right]} \quad (13b)$$

In general, j_a , j_w and j_o are the control parameters and are thus known. Hence, $\langle \alpha_a \rangle$, $\langle \alpha_w \rangle$ and $\langle \alpha_o \rangle$ can be determined by using Eqs. 1, 11 and 12 and 3, if the related phase distribution parameters (C_a , C_w and C_o) and drift velocities (V_{aj} , $V_{w\ell}$ and $V_{o\ell}$) are known.

Experimental Data

The experimental data taken in this study are given in Tables 1. When these data are classified according to the flow regimes shown schematically in Figure 2 (Açıkgöz et al., 1992), and plotted in the so-called drift-flux plane, flow regime specific values for the phase distribution parameter (that is, the slope) and the drift velocity (that is, the intercept) result. Figures 3–

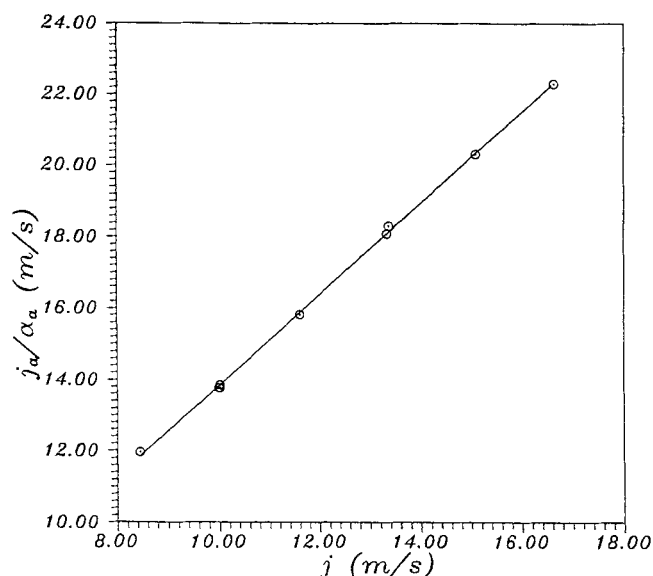


Figure 17. Drift-flux plot, oil-based stratifying-annular flow: region-6.

($C_a = 1.359$, $V_{aj} = -0.319$ cm/s).

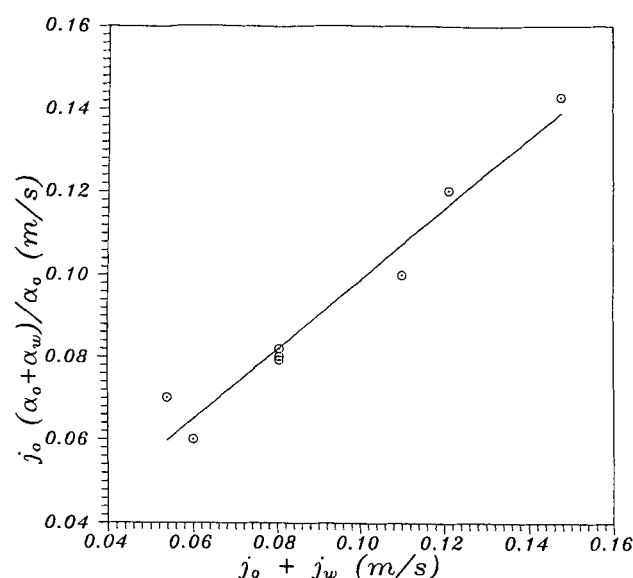


Figure 18. Drift-flux plot, oil-based stratifying-annular flow: region-6.

($C_o = 1.002$, $V_{ot} = 0.000$ cm/s).

18 show that these data are well correlated by the generalized three-phase drift-flux model derived herein for both oil-based and water-based stratified/wavy, plug, slug, and annular flow regimes.

It is interesting to note that, as expected, for horizontal three-phase flows the drift velocities are normally quite small, indicating relatively little local slip compared to vertical flows. Moreover, it was found that the stratified/wavy type flow regimes 3&4 (oil-based) and 8&9 (water-based), shown schematically in Figure 2, could be grouped together when the drift-flux parameters were determined.

For the reader's convenience, the drift-flux parameters which were determined graphically are summarized in Table 2. It can be seen that, as for two-phase flows, there can be a significant variation in the drift-flux parameters from one flow regime to

the other. Moreover, the appropriate values of these drift-flux parameters may be different for other fluids, larger conduit sizes, and other system pressures. Thus in order to deduce reliable design correlations (for example, for use in undersea oil well technology) more data are needed in larger diameter conduits and at higher system pressures. Nevertheless, this study has clearly shown that three-phase data in horizontal conduits can be correlated using drift-flux techniques; an observation which opens the way for significant advances in the field of three-phase flow technology.

Conclusions

It has been shown that drift-flux models can be used for gas/water/oil horizontal three-phase flows. In order to be able

Table 2. Drift-Flux Parameters for Various Flow Regimes

Water-Based Flow Regimes					
Drift-Flux Parameters	Dispersed Slug Flow (Region 7)	Stratified/ Wavy & Incipient Annular Flows (Regions 8 & 9)	Dispersed Stratifying-Annular Flow (Region 10)		
C_a	1.289	1.115	1.041		
V_{aj} (cm/s)	-0.096	0.725	1.218		
C_w	1.049	1.056	1.047		
V_{wt} (cm/s)	-0.025	-0.023	-0.028		
Oil-Based Flow Regimes					
Drift-Flux Parameters	Dispersed Plug Flow (Region 1)	Dispersed Slug Flow (Region 2)	Stratified/ Wavy Flows (Regions 3 & 4)	Wavy/ Stratifying-Annular Flow (Region 5)	Stratifying-Annular Flow (Region 6)
C_a	1.514	2.328	1.084	1.501	1.359
V_{aj} (cm/s)	0.184	-0.270	2.016	1.093	-0.319
C_o	0.914	0.938	1.038	1.084	1.002
V_{ot} (cm/s)	0.008	-0.008	0.002	-0.008	0.000

to predict the global volumetric phase fractions of the liquid phases, new liquid/liquid drift-flux parameters were derived. In contrast, drift-flux parameters similar to those used in two-phase flow were found to be valid for the gas phase in three-phase flows. Experimental data have been taken which verify the validity of drift-flux models for horizontal three-phase flows. It appears that the flow-regime-specific drift-flux parameters determined in this study can be generalized for use in undersea oil well technology, but this will require the acquisition of more prototypic three-phase flow data in larger diameter conduits and at higher system pressures.

Notation

- α_k = volume fraction of phase-k
 C_k = phase distribution parameter for phase-k
 j = total volumetric flux ($j_a + j_w + j_o$)
 j_k = volumetric flux of phase-k
 V_{aj} = drift velocity between air and the volumetric flux of the air/water/oil mixture
 V_{wf} = drift velocity between water and the volumetric flux of the water/oil mixture
 V_{of} = drift velocity between the oil and the volumetric flux of the water/oil mixture
 $\langle \zeta_k \rangle$ = cross-sectional average of parameter ζ_k

Subscripts

- a = air
 o = oil
 w = water

Literature Cited

- Açıkgöz, M., R. T. Lahey, Jr., and F. França, "An Experimental Study of Three-Phase Flow Regimes," accepted for publication, *Int. J. of Multiphase Flow*, **18**(3), 327 (1992).
 Bhaga, D., and M. E. Weber, "Holdup in Vertical Two and Three-Phase Flow, Part I and II," *Canadian J. of Chem. Eng.*, **50**, 323 (1972).
 França, F., and R. T. Lahey, Jr., "The Use of Drift-Flux Techniques for the Analysis of Horizontal Two-Phase Flows," to be published, *Int. J. of Multiphase Flow* (1992).
 Galyamov, M. N., and N. L. Karpshin, "Change in the Viscosity of the Liquid Phase During the Movement of Gas-Water-Oil Mixtures in Pipelines," *Transport i Khranenie i Nefteproductov*, **2**, 14 (1971).
 Shean, A. R., "Pressure Drop and Phase Fraction in Oil-Water-Air Vertical Pipe Flow," MS Thesis, Massachusetts Institute of Technology (1976).
 Tek, R. M., "Multiphase Flow of Water, Oil and Natural Gas Through Vertical Flow Strings," *J. of Petrol. Techn.*, 1029 (1961).
 Zuber, N., and J. A. Findlay, "Average Volumetric Concentration in Two-Phase Flow Systems," *J. of Heat Transfer*, 453 (Nov., 1965).

Manuscript received Oct. 30, 1991, and revision received Apr. 23, 1992.